www.czasopisma.pan.pl PAN POLSKA AKADEMIA NAUK www.journals.pan.pl

Arch. Metall. Mater. **65** (2020), 4, 1391-1396

DOI: 10.24425/amm.2020.133705

B. GARBARZ-GLOS[1*], W. BĄK[1], A. BUDZIAK[2], P. DULIAN[3], A. LISIŃKA-CZEKAJ[4], D. CZEKAJ[4]

THE APPLICATION OF THE MECHANOCHEMICAL SYNTHESIS FOR THE PREPARATION OF ADVANCED CERAMICS BASED ON BARIUM TITANATE

In the present study, the lead-free $BaTi_{1-x}Zr_xO_3$ (for x = 0, 0.05 and 0.15) ceramics were prepared by High-Energy Ball Milling and heat treatments. The performed X-ray, SEM and EDS measurements confirmed high purity, good quality and the expected quantitative composition of the obtained samples. The study of dielectric properties was performed by means of broadband dielectric spectroscopy at the frequency ranging from 0.1 Hz to 10 MHz. The obtained measurement data, analyzed in accordance with the Arrhenius formalism demonstrated the presence of relaxation type dielectric mechanisms. The impedance answer of studied ceramic materials indicated the presence of two relaxation processes: one with a dominant resistive component and the other with a small capacitive component. The observed dielectric relaxation process is temperature dependent and has a "non-Debye" character.

Keywords: $BaTiO_3$, Mechanochemical synthesis, X-ray methods, Dielectric properties

1. Introduction

From technological point of view, the mechanochemical synthesis is one of the often applied methods in the synthesis of ceramic materials. It allows to obtain ceramic materials with optimal and well-defined electrophysical properties. Moreover, mechanochemical synthesis, which is a low-temperature solid state processing technique, enables a strict control of stoichiometry and eliminates undesirable losses of volatile elements [1-4]. One of the ABO_3 oxides with a perovskite type structure material, obtained by this method, is $BaTi_{1-x}Zr_xO_3$ solid solutions. The basic compounds: barium titanate $BaTiO_3$ and barium zirconate $BaZrO_3$, as well as the solid solution based on these compounds (obtained by a conventional solid state reaction method) have been extensively studied in both experimental and theoretical aspects [5-12]. A very useful method for the electrical characterization of this type of materials is broadband dielectric spectroscopy. This method, using the appropriate data analysis, makes it possible to characterize the electrically varied active regions in the material both qualitatively, by showing their existence, and quantitatively, by measuring their individual electric properties [13-15]. Formally, the experimental electrical output response may be described by complex functions: electric permittivity, electric modulus, as well as impedance and admittance. The interpretation of frequency-dependent complex impedance can be executed by various models [16-18]. The novelty objective of this work is obtaining barium titanate-based materials containing zirconium using a mechanochemical synthesis based on the high-energy ball milling technique, as well as to investigate the effect of synthesis condition on the structural, microstructural and dielectric properties of the received materials.

2. Experimental procedure

2.1. Preparation

The $BaTi_{1-x}Zr_xO_3$ (for x = 0, 0.05 and 0.15; hereafter in the text abbreviated as BT, BTZ05 and BTZ15) ceramic samples were prepared with the use of the high-energy ball milling technique (HEBM). Barium oxide BaO (Sigma Aldrich, 90%), titanium dioxide TiO_2 (Evonik Degussa P25 GmbH, 98.0%) and zirconium oxide ZrO_2 (Alfa Aesar, 99.5 %) were used as the primary raw materials. These precursors of stechiometric

[1] INSTITUTE OF TECHNOLOGY, PEDAGOGICAL UNIVERSITY OF CRACOW, 2 PODCHORĄŻYCH STR., 30-084 KRAKÓW, POLAND
[2] AGH UNIVERSITY OF SCIENCE AND TECHNOLOGY, FACULTY OF ENERGY AND FUELS, AL. MICKIEWICZA 30, 30-059 KRAKÓW, POLAND
[3] CRACOW UNIVERSITY OF TECHNOLOGY, FACULTY OF CHEMICAL ENGINEERING AND TECHNOLOGY, 24 WARSZAWSKA STR., 31-155 KRAKÓW, POLAND
[4] GDAŃSK UNIVERSITY OF TECHNOLOGY, FACULTY OF MECHANICAL ENGINEERING, DEPARTMENT OF MATERIALS ENGINEERING AND WELDING, 11/12 G. NARUTOWICZA STR., 80-233, GDAŃSK, POLAND

* Corresponding author: barbara.garbarz-glos@up.krakow.pl

quantity were subjected to a high-energy milling in a Fritsch GmbH Pulverisette 6 planetary ball mill. The milling was performed in air with a vessel and balls (φ = 10 mm) made of ZrO_2. The vessel was rotated at 500 rpm for 1.5 hours with a ball-to-powder weight ratio (BPR) of 20:1. The milled powders were compacted and sintered at the temperature of 1620 K for 3 h. For a high-temperature synthesis, the appropriate amounts of raw materials were mixed and pressed into pellet discs with the diameter of 8 mm.

2.2. Equipment

The X-ray studies of the $BaTi_{1-x}Zr_xO_3$ ceramics were performed by means of an X'Pert PRO (PANalytical) diffractometer with the Cu-Ka radiation (λ = 1.5406 Å) and a graphite monochromator. The sample was placed in a nickel-plated copper sample holder of dimensions 18×9×0.2 mm^3. The temperature of the sample was stabilized (an accuracy ±0.1 K) with a continuous flow cryostat supplied by Anton Paar Co. Prior to the temperature measurements the sample was melted, next cooled to the liquid nitrogen temperature with the rate of 0.16 K/s. The X-ray diffraction patterns were obtained at the rising temperature. After each heating stage, the sample was allowed to equilibrate for about 600 s. Data were obtained using automatic slits and subsequently recalculated to the fixed slits mode. All analysed patterns were made in the wide angle range of 2 theta from 10 to 100 degrees. A profile-fitting program Fullprof [19] based on the Rietveld method was used to analyse and fit the X-ray patterns. The microstructure analysis and the investigations of chemical composition were performed using a Hitachi S4700 scanning electron microscope (SEM) equipped with an Oxford Instruments Energy Dispersive X-Ray Spectroscopy (EDS) stage. The use of a lithium-drifted siliceous detector with a multichannel pulse height analyzer enabled to obtain the diffraction patterns in chosen surface microregions of the sample. The EPMA (Electron Probe Microbeam Analysis) was applied to the analysis of elements distribution on the sample surface. All the samples for the SEM/EDS/EPMA analysis were cut to give cross sections, and polished using abrasives. The dielectric studies were carried out using a Novocontrol System consisting of an Alpha-AN High Performance Frequency Analyzer combined with a cryogenic temperature control system – Quatro Cryosystem (the temperature was controlled with the accuracy of ±1 K). The measurements were made in the temperature range from 140 K to 600 K. The frequencies varied from 0.1 Hz to 10 MHz at the applied voltage 1 V. Nitrogen gas was used as a heating and cooling agent. Prior to all measurements, the samples were maintained at 450 K for 1 hour in order to eliminate internal and near electrode stresses.

3. Results and discussion

The XRD analysis confirmed the formation of a perovskite structure in the $BaTi_{1-x}Zr_xO_3$ solid solution. A shift in the diffraction peaks towards lower angles with comparison to the pure barium titanate $BaTiO_3$ with the Zr-substitution up to x = 0.15 are observed (Fig. 1). This behaviour indicates, that the values of the lattice parameters in BTZ05 and BTZ15 samples increased. The increase may be explained by the difference in the radius and electronic density of Ti^{4+} and Zr^{4+} ions. It should be pointed that Zr^{4+} ions have a larger ionic size (0.0720 nm) than the titanium ions Ti^{4+} (0.0605 nm) [20]. Due to this fact, the substitution of Ti^{4+} with Zr^{4+} leads to an expansion of unit cell. From the obtained results for room temperature, the elementary cell parameters *a* were determined: 4.00689 Å, 4.01669 Å and 4.0334 Å for BT, BTZ05 and BTZ15 respectively.

The analysis of cell parameter *a* for BT, BTZ05 and BTZ15 were performed in the temperature range from 140 to 440 K. The results are presented in Figure 2.

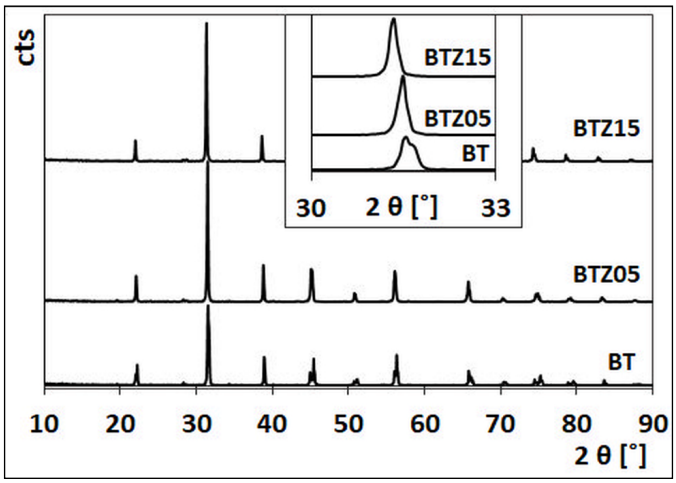

Fig. 1. XRD patterns of $BaTi_{1-x}Zr_xO_3$ ceramics at room temperature

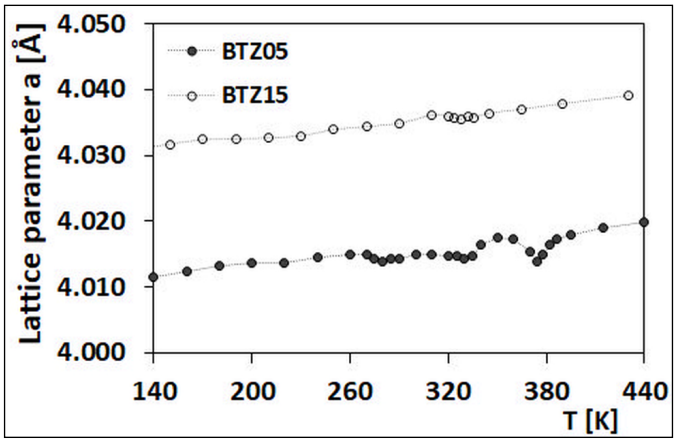

Fig. 2. The lattice parameter *a* vs. temperature obtained for the ceramic samples BTZ05 and BTZ15

Based on the obtained X- ray diffraction patterns, the phase analysis has been performed, which also confirmed three phase transitions: around (T_1) 280 K (rhombohedral → orthorombic), around (T_2) 328 K (orthorombic → tetragonal) and tetragonal → cubic phase transition around (T_c) 373 K in the case of BTZ05. At the temperature of ~328 K the small anomaly in

the temperature dependence of $a(T)$ for BTZ15 is visible. This point characterizes the rhombohedral-cubic structural transition. Moreover, the anomaly mentioned above occurs also in the temperature dependence of real part of complex dielectric permittivity and is related to the ferroelectric-paraelectric phase transition (Fig. 3). When the Zr^{4+} ion is substituted in the sublattice site, the Curie temperature (T_c) is shifted towards lower values of temperature [21]. The other two low-temperature (T_1, T_2) transitions observed for pure $BaTiO_3$, from a tetragonal to orthorhombic structure and from an orthorhombic to rhombohedral phase are shifted to higher temperatures with the increase of zirconium content. For zirconium concentration x = 0.15, all three phase transition temperatures corresponding to pure barium titanate are merged into a single phase transition and the so-called pinching effect takes place [11,22].

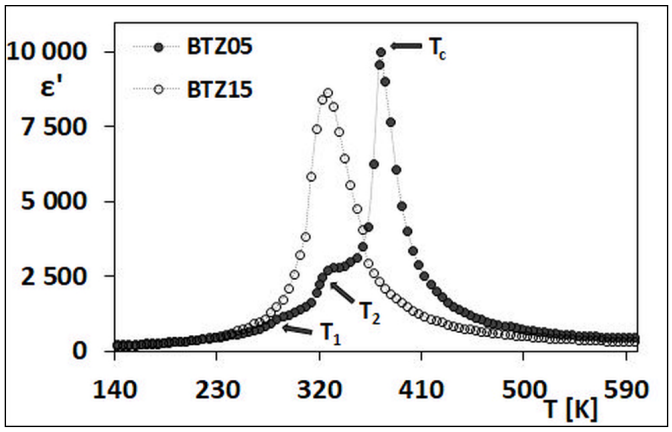

Fig. 3. The temperature dependence of the real part of the complex dielectric permittivity for BTZ05 and BTZ15 samples (f = 1 MHz)

The micrographs of the BTZ05 and BZT15 ceramics obtained by the SEM investigation are presented in Figure 4a and Figure 4b. The images show a homogeneous and fine-grained microstructure (polyhedral-shaped grains are visible) with very a small degree of porosity. The growth terraces are seen, which indicates that the growth of grains occurred according to a layer mechanism with a screw dislocation.

The local analysis of the chemical composition (by means of EDS) confirmed the high purity and the expected qualitative composition. Moreover, the investigation of element distribution in the samples (carried out by an EPMA method using an X-ray microprobe) confirmed the qualitative composition of the BTZ05 and BZT15 samples. To determine the average crystallite size of the investigated samples the Scherrer equation [23] was used. The zirconium additive causes an increase the size of the grain. It was found that the average crystallite sizes for doped ceramics are included in the range from 11 μm to 13 μm (for the $BaTiO_3$ sample prepared by a HEBM method, the average size of about 9 mm is noticeable – Figure 4c). Figure 5 presents the frequency dependence of the imaginary parts of the impedance (Z'') for the BTZ05 and BTZ15 ceramics at chosen temperatures. The analysis of $Z''(f)$ plots shows the appearance of two maxima. These maxima indicate that there are two relaxation

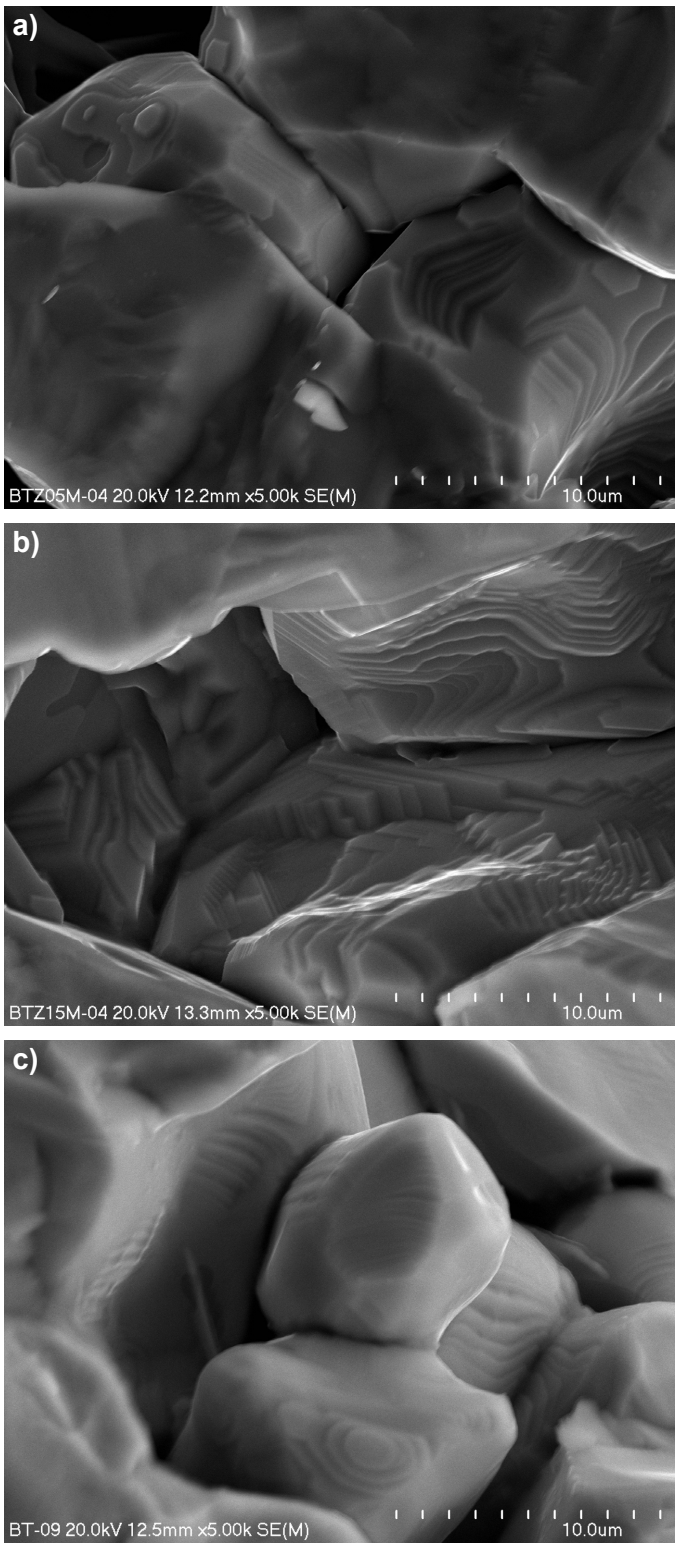

Fig. 4. SEM micrographs of the fractured surface of samples BTZ05 (a), BZT15 (b) and BT (c); magn. 5 000×

mechanisms due to the occurrence of both the grain and grain boundary [24]. The low frequency maximum can be assigned to the grain boundary effect, whereas at the high frequency side, the maximum corresponds to contributions of the grain (bulk) in relaxation process. In addition, the shift of the maximum values of the impedance Z" towards higher frequencies with increasing temperature signifies that the relaxation times are decreasing.

The observed decrease in the value of impedance with increasing temperature is understood on the basis of a thermal activation of charge carriers. The peak broadening, likewise, indicates the presence of temperature dependent electrical relaxation phenomenon, in which the relaxation may be caused by the presence of electrons at lower temperatures and defects or vacancies at higher temperatures.

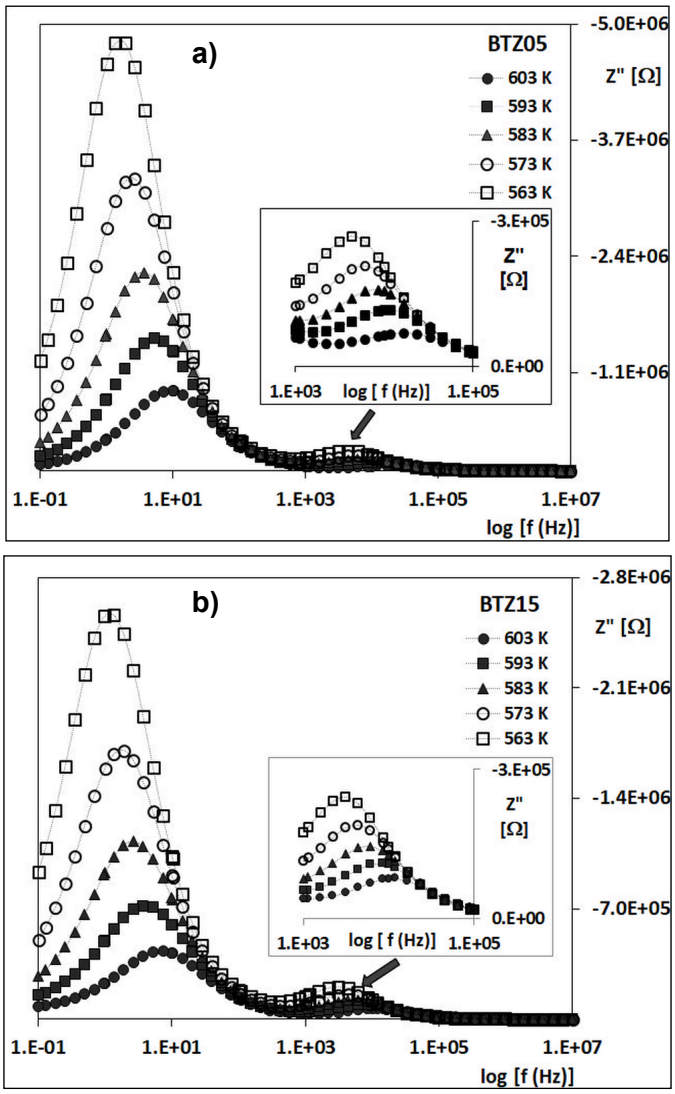

Fig. 5. The imaginary part of the impedance as a function of the frequency for BTZ05 (a) and BTZ15 (b) samples at various temperatures

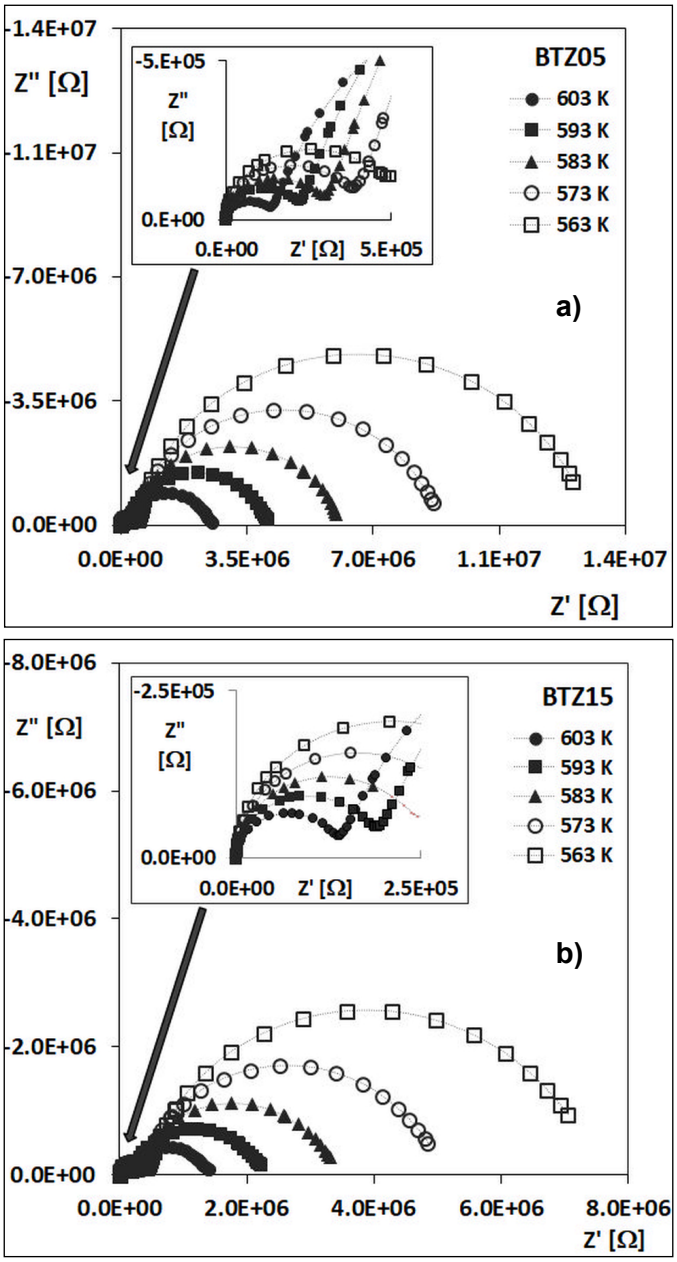

Fig. 6. The Nyquist diagrams of the complex impedance for BTZ05 (a) and BTZ15 (b) ceramics at various temperatures

Figure 6 presents the Nyquist diagrams (Z'' vs. Z') for BTZ05 and BTZ15 ceramic materials. The occurrence of the semicircular arcs is associated with the existence of regions with a diverse electrical activity. The weaker high-frequency process can be attributed to the grain (bulk) impedance response, and the stronger one to the low frequency, originating from the free charge and the induced polarization occurring on grain boundaries.

The position of the intersection point of the semicircular arcs with the real axis of the impedance shifts to the low values of Z' with increasing temperature. The temperature increase also causes the decrease in the experimentally observed semicircle radiuses for all investigated samples. Such behaviour suggests that the relaxation times of electrical processes change with temperature in the investigated frequency range. The relaxation time τ for the grain and grain boundary can be calculated from the relation $2\pi f_m \tau = 1$, where the f_m is the frequency of the maximum of $Z''(f)$ function. The activation energy was determined from the equation [25,26] which is valid for the Debye-like loss mechanisms: $\tau = B\exp(E_a/k_B T)$; here B is a pre-exponential factor, and k_B is a Boltzmann constant ($8.314 \cdot 10^{-5}$ eV/K) and T have their usual significance. The thermally activation energy of the relaxation processes for grain (bulk) and grain boundary were calculated and given in Figure 7.

The activation energies for the grain boundaries (highly defective regions that separate the one grain from another) are greater than the grain contribution, thus we are dealing with

the resistive nature of grain boundaries. These values point out the fact that the conduction mechanism for the investigated ceramics in the same measured temperature range is mainly dominated by the grain boundary conduction process involving the hopping electrons [27] created due to the oxygen vacancies according to the Kröger and Vink equation [28]. In the barium titanate based solid solutions, different point defects generated during a manufacturing process may occur. These include the native structural defects in the subnets A, B, and O in the form of vacancies or interstitial ions [29,30]. It is known that in the case of barium titanate, the electrical properties are primarily related to the oxygen nonstoichiometry. Their concentration can be varied by the selection of appropriate parameters during the technological process (the processing of any advanced ceramics plays a significant role in determining the properties and performance of the final product). In the case of the mechanochemical synthesis, the milling process results in mechanical stresses, which lead to elastic and inealastic deformation of the particles. The application of mechanical energy gives rise to the changes in other physical properties of particles, such as the increase in localized temperature, lattice rearrangements within the particle and creation of various defects [3,31].

4. Conclusions

The barium zirconium titanate samples $BaTi_{1-x}Zr_xO_3$ for x = 0, 0.05, and 0.15 were prepared with the use of the high-energy ball milling technique (HEBM). The structure and morphology of BTZx samples were monitored using X-ray diffraction (XRD) and scanning electron microscopy (SEM). The X-ray measurements confirmed the mono-phase character of the samples as well as the chemical composition according to the assumed standards. Moreover the difference in the average radius of cations in the B site size, $r(Zr^{4+}) = 0.0730$ nm and $r(Ti^{4+}) = 0.0605$ nm created the difference in the unit cell parameters. The performed SEM and EDS studies revealed that the material is characterized by high density, homogeneity of microstructure, polyhedral shape of grains and low porosity. It was also found that the substitution of Zr^{4+} for Ti^{4+} in $BaTiO_3$ resulted in shifting two low-temperature transitions (T_1, T_2) of the investigated samples to higher temperatures and decreasing the tetragonal-cubic phase transition temperature (T_c) (this so-called pinching effect is confirmed also by earlier studies carried out and described by authors conducting dielectric measurements). The application of broadband dielectric spectroscopy made it possible to characterize and separate the dielectric properties of the grains and grain boundaries. The thermally activation energies of the relaxation processes related to the electric conductivity for the grains and grain boundaries were calculated. It was also pointed that the fluctuation of chemical composition in the microregions of ceramics associated with the distribution ("disorder") of cations in the B sublattice is one of the sources of relaxation effects observed in the studied materials.

REFERENCES

[1] P. Baláž, M. Achimovičová, M. Baláž, P. Billik, Z. Cherkezova-Zheleva, J.M. Criado, F. Delogu, E. Dutková, E. Gaffet, F.J. Gotor, R. Kumar, I. Mitov, T. Rojac, M. Senna, A. Streletskii, K. Wieczorek-Ciurowa, Hallmarks of mechanochemistry: From nanoparticles to technology, Chem. Soc. Rev. **42**, 7571-7637 (2013).

[2] M. Sopicka-Lizer, High-Energy Ball Milling: Mechanochemical Processing of Nanopowders, CRC Press, Boca Raton USA, (2010).

[3] L.B. Kong, T.S. Zhang, J. Ma, F. Boey, Progress in synthesis of ferroelectric ceramic materials via high energy machanochemical technique, Prog. Mater. Sci. **53**, 207-322 (2008).

[4] K. Wieczorek-Ciurowa, P. Dulian, W. Bąk, C. Kajtoch, High-energy ball milling as a green chemistry method for modification of $CaTiO_3$ electrical properties, Przemysł Chemiczny **90**, 1400-1403 (2011).

[5] S. Parida, S.K. Rout, L.S. Cavalcante, E. Sinha, M. Siu Li, V. Subramanian, N. Gupta, V.R. Gupta, J.A. Varela, E. Longo, Structural refinement, optical and microwave dielectric properties of $BaZrO_3$, Ceram. Int. **38**, 2129-2138 (2012).

[6] J.R. Tolchard, T. Grande, Chemical compatibility oxide cathodes for $BaZrO_3$ electrolytes, Solid State Ionics **178**, 593-599 (2007).

[7] R. Khenata, M. Sahnoun, H. Baltache, M. Rerat, A.H. Rashek, N. Illes, B. Bouhafs, First principle calculations of structural, electronic and optical properties of $BaTiO_3$ and $BaZrO_3$ under hydrostatic pressure, Solid State Commun. **136**, 120-125 (2005).

[8] C. Ciomaga, M. Viviani, M.T. Buscaglia, V. Buscaglia, L. Mitoseriu, A. Stancu, P. Nanni, Preparation and characterisation of the $Ba(Zr,Ti)O_3$ ceramics with relaxor properties, J. Eur. Ceram. Soc. **27**, 4061-4064 (2007).

[9] B. Garbarz-Glos, W. Śmiga, R. Bujakiewicz-Korońska, W. Suchanicz, M. Dambekalne, M. Livinsh, A. Sternberg, Influence of zirconium on structural, microstructural and ferroelectric properties of $BaZr_{0.20}Ti_{0.80}O_3$ ceramic, Int. Ferroelectrics **108**, 67-76 (2009).

[10] B. Garbarz-Glos, R. Bujakiewicz-Korońska, D. Majda, M. Antonova, A. Kalvane, C. Kuś, Differential scanning calorimetry investigation of phase transition in $BaZr_xTi_{1-x}O_3$, Integr. Ferroelectr. **108**,106-115 (2009).

[11] Z. Yu, C. Ang, R. Guo, A.S. Bhalla, Dielectric properties of $Ba(Ti_{1-x}Zr_x)O_3$ solid solution, Mater. Lett. **61**, 326-329 (2007).

[12] V.V. Shvartsman, J. Zhai, W. Kleemann, The dielectric relaxation in solid solutions $BaTi_{1-x}Zr_xO_3$, Ferroelectrics **379**, 77-85 (2009).

[13] J.E. Bauerle, Study of solid electrolyte polarization by a complex admittance method, J. Phys. Chem. Solids **30**, 2657- 2670 (1969).

[14] E.J. Abram, D.C. Sinclair, A.R. West, A strategy for analysis and modelling of impedance spectroscopy data of electroceramics: doped lanthanum gallate, J. Electroceram. **10**, 165-177 (2003).

[15] N. Hirose, A.R. West, Impedance spectroscopy of undoped $BaTiO_3$ ceramics, J. Am. Ceram. Soc. **79**, 1633-1641 (1996).

[16] K. Cole, R. Cole, Dispersion and absorption in dielectrics. I. Alternating current characteristics, J. Chem. Phys. **9**, 341-352 (1941).

[17] D. Davidson, R. Cole, Dielectric relaxation in glycerol, propylene glycol, and n-propanol, J. Chem. Phys. **19**, 1484-1490 (1951).

[18] S. Havriliak, S. Negami, A complex plane representation of dielectric and mechanical relaxation processes in some polymers, Polymer **8**, 161-210 (1967).

[19] J. Rodriguez-Carvajal, Fullprof: A Program for Rietveld Refinement and Pattern Matching Analysis, Abstract of the Satellite Meeting on Powder Diffraction of the XV Congress of the IUCr, Toulouse, France, 127-132 (1990).

[20] R.D. Shannon, Revised effective ionic radii and systematic studies of interatomic distances in halides and chalcogenides, Acta. Crystallogr. A. **32**,751-926 (1976).

[21] P. Dulian, B. Garbarz-Glos, W. Bąk, M. Antonova, C. Kajtoch, K. Wieczorek-Ciurowa, H. Noga, Dielectric behaviour of ceramics obtained by means of solid state and mechanochemical synthesis, Ferroelectrics **497**, 1-7 (2016).

[22] B. Garbarz-Glos, AC impedance spectroscopy study of $BaZr_{0.10}Ti_{0.90}O_3$ ceramics, Ferroelectrics **486**, 1-7 (2015) .

[23] J.I. Langford, A.J.C. Wilson, Scherrer after sixty years: A survey and some new results in the determination of crystallite size, J. Appl. Crystallogr. **11**, 102-113 (1978).

[24] D.C. Sinclair, A.R. West, Impedance and modulus spectroscopy of semiconducting $BaTiO_3$ showing positive temperature coefficient of resistance, J. Appl. Phys. **66**, 3850-3863 (1989).

[25] P. Debye, Polar Molecules, Dover Publications, New York (1959).

[26] H. Fröhlich, Theory of dielectrics, Dielectric constant and loss, Oxford University Press, London (1958).

[27] H. Böttger, V.V. Bryksin, Hopping Conduction in Solids, Akademie-Verlag, Berlin (1985).

[28] H.J. Hagemann, D. Hennings, J. Am. Ceram. Soc. **64**, 590-594 (1981).

[29] K. Tkacz-Śmiech, A. Koleżyński, W.S. Ptak, Ferroelectrics **237**, 57-64 (2000).

[30] K. Tkacz-Śmiech, A. Koleżyński, W. Jastrzębski, Ferroelectrics **315**, 73-81 (2005).

[31] V. Sepelak, A. Duevel, M. Wilkening, K.D. Becker, P. Heitjans, Chem. Soc. Rev. **42**, 7507-7520 (2013).